Strong self- and cross-phase modulation effects in chromium-doped $KTiOPO_4$ crystals

E. Jurdik[a)]
Research Institute for Materials, University of Nijmegen, Toernooiveld 1, 6525 ED Nijmegen, The Netherlands

A. V. Petukhov[b)]
Research Institute for Materials, University of Nijmegen, Toernooiveld 1, 6525 ED Nijmegen, The Netherlands and NSR Research Center, University of Nijmegen, 6525 ED Nijmegen, The Netherlands

A. Anema, A. van Etteger, and Th. Rasing
Research Institute for Materials, University of Nijmegen, Toernooiveld 1, 6525 ED Nijmegen, The Netherlands

(Received 4 December 2000; accepted for publication 10 May 2001)

The presence of chromium impurities in the crystal matrix of chromium-doped $KTiOPO_4$ is shown to be at the origin of a strong cubic optical nonlinearity of this material. As a result, a pronounced self-phase modulation of a Gaussian laser beam at 532 nm is observed in the far field as a diffraction pattern consisting of alternating dark and bright rings. The induced nonparabolic and polarization sensitive refractive index change is also used to modulate a weak probe laser beam at 633 nm. A simple theoretical model incorporating a laser heating process and a thermo-optical effect accounts for the main features observed in our experiments and elucidates the mechanisms leading to the diffraction pattern formation. © *2001 American Institute of Physics.* [DOI: 10.1063/1.1383979]

I. INTRODUCTION

Potassium titanyl phosphate ($KTiOPO_4$ or KTP) is a material exhibiting superior properties for nonlinear optical applications, such as second harmonic generation and electro-optics.[1–3] For a number of applications it is desirable to alter and control its physical properties. This goal can be achieved by, for example, incorporation of trivalent cations into the crystal lattice of KTP. It was shown that doping with Al^{3+}, V^{3+}, Ga^{3+}, and Cr^{3+} reduces the ionic conductivity and the optical damage threshold of KTP.[4,5] In addition, spectroscopic properties of KTP are changed due to the presence of impurities.[4,6,7] The absorption and luminescence of, for example, Cr:KTP have indicated the possibility of using this crystal as an active medium in a self-frequency doubling laser.[6] Also, it has been shown that another crystal, Ce:KTP, has lower absorption coefficients compared with undoped KTP, resulting in more efficient blue light generation from this material.[7] Very recently, the influence of impurities on ultraviolet optical damage of KTP was studied.[8]

When an intense laser beam propagates through a nonlinear medium, it can induce large changes of the cubic dielectric properties that in turn affect the beam propagation itself. Extensive theoretical and experimental investigations of these self-phase modulation effects have been performed over the past two decades (for a review, see Ref. 9). For a large laser-induced refractive index, the self-action of the laser beam can result in a far field diffraction pattern. A number of materials were found to exhibit a very pronounced cubic nonlinearity. These include solids, liquids, liquid crystals, and gases. Moreover, two laser beams can couple to each other via the cubic susceptibility. This cross-phase modulation effect can be used to alter propagation of low intensity beams.

In this article, we show that a strong cubic nonlinearity is induced by the presence of Cr^{3+} ions in the crystal matrix of KTP. When Cr:KTP is irradiated with a continuous wave (cw) laser beam with a wavelength within its absorption band, a strong self-phase modulation takes place. This manifests itself in the far field as a diffraction pattern consisting of dark and bright rings. A cross-phase modulation effect is also demonstrated by altering the spatial profile of a second laser beam with another wavelength. We present a simple theoretical model based on a laser heating process and a thermo-optical effect. This model is able to reproduce the main features observed in our experiments and can serve as a useful guide for further investigations.

II. SELF-DIFFRACTION

The Cr:KTP crystals for this work were grown from a high-temperature solution of TiO_2 and $K_6P_4O_{13}$. In order to introduce Cr into the crystal structure, a small fraction of TiO_2 was replaced by CrO_2. This approach resulted in high quality single crystals of typical dimensions $7\times4\times5(x\times y\times z)$ mm^3. Several crystals with three different doping concentrations of 185 parts per million (ppm), 233 and 677 ppm, respectively, cut along three crystallographic directions and polished on all six sides were used for further optical investigations. Here, mainly the results obtained with the heaviest doped crystals (677 ppm) are reported.

The cw laser beam used in our experiments was a Gaussian mode of a diode-pumped, frequency-doubled Nd:YVO_4

a)Electronic mail: ejurdik@sci.kun.nl
b)On leave from the Institute of Crystallography, 117333 Moscow, Russia.

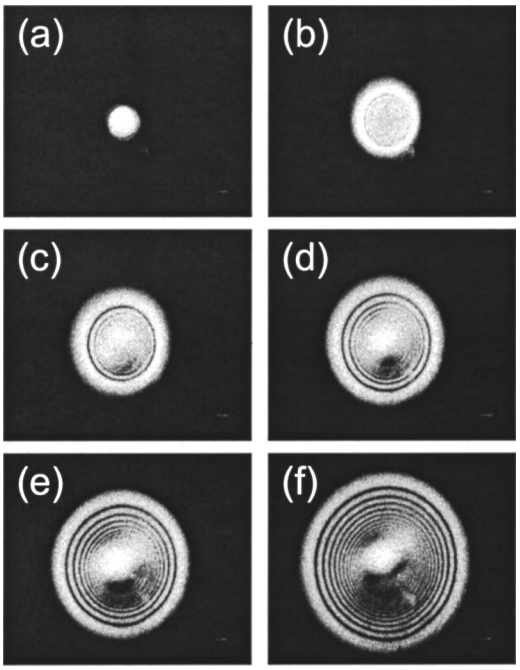

FIG. 1. Self-induced diffraction patterns from a 677 ppm Cr:KTP crystal for a *z* polarized, propagating along *y* laser beam at 532 nm focused by a 200 mm positive lens onto the crystal. The laser power was (a) 200 mW, (b) 750 mW, (c) 900 mW, (d) 1000 mW, (e) 1100 mW, and (f) 1200 mW.

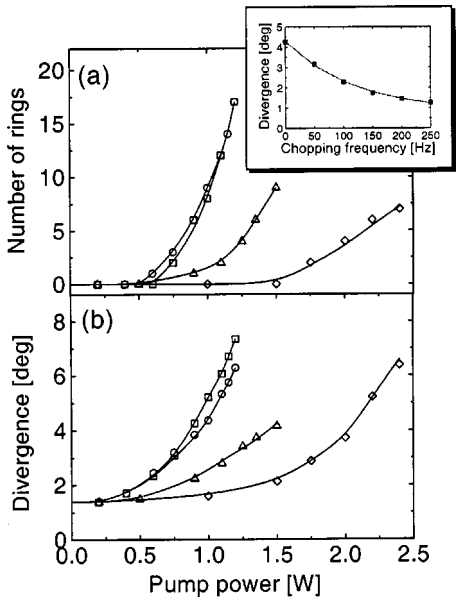

FIG. 2. The number of bright diffraction rings (a) and the outermost ring divergence (b) as a function of the laser power for different polarization and propagation directions for a 677 ppm Cr:KTP crystal (the lines are guides for the eyes). Polarization *z*-propagation *y* (□), *z*-*x* (○), *y*-*x* (△), and *x*-*y* (◇). The inset shows the evolution of the beam diameter as a function of the chopping frequency for a laser power of 900 mW. An exponential fit to this dependence revealed a response time of 4 ms.

laser at a wavelength of 532 nm. The laser polarization was linear and its orientation could be adjusted with a half wave plate. The laser beam was focused onto the crystal by a 200 mm positive lens, resulting in a $1/e^2$ beam radius of approximately 30 μm. After passing through the crystal, the beam was projected onto a white screen 1.8 m from the sample and the image was recorded with a charge-coupled device camera. Also, the laser beam propagation inside the crystal was monitored with an optical microscope.

For all available Cr:KTP samples, the laser beam profile and divergence substantially depended on the incident light intensity and polarization. As an example, Fig. 1 shows a series of snapshots demonstrating a striking sensitivity of the intensity profile on the laser power P for polarization along the *z* axis and propagation along the *y* axis of a 677 ppm Cr:KTP. Initially, for $P=200$ mW [Fig. 1(a)], the laser beam divergence was not influenced by the presence of the nonlinear material. As P was increased, the beam divergence smoothly increased and the on-axis laser beam intensity decreased. At $P=750$ mW, the first dark diffraction ring appeared [Fig. 1(b)]. Further increase in P resulted in a rapid increase of the number of diffraction rings [Figs. 1(c)–1(e)], reaching a maximum of 17 bright rings at $P=1200$ mW [Fig. 1(f)]. For even higher laser powers, the diffraction pattern became unstable and eventually resulted in violent breakdown of the crystal.

The evolution of the laser beam shape in the crystal was observed with an optical microscope. As the first dark diffraction ring appeared, a self-focus was noticed inside the crystal near its output face. With increasing laser power, this self-focus moved towards the input face where the light intensity could reach extremely high values (about 10^6 W/cm^2) and thus cause material damage.

The phenomenon of self-diffraction in Cr:KTP must be connected with the presence of impurities, as we did not observe it in pure KTP crystals. In order to identify the processes leading to the ring formation, we made use of the biaxial nature of Cr:KTP and the fact that crystals with three different doping rates were available. For a wavelength of 532 nm, the measured absorption coefficients along the three crystallographic directions *x*, *y*, and *z* of 677 ppm Cr:KTP are 1.3, 1.9, and 3.4 cm^{-1}, respectively (see also Ref. 6). Figures 2(a) and 2(b) show the number of bright diffraction rings and the outermost ring divergence, respectively, as functions of the laser power for all three respective polarization directions for a 677 ppm Cr:KTP crystal. Clearly, the absorption plays a key role in self-diffraction from Cr:KTP, with the *z* polarized laser beam exhibiting the most pronounced effect. Also, the role of the propagation direction was investigated. For a polarization along the *z* axis two curves (corresponding to propagation along *x* and *y*, respectively) are shown in Fig. 2. Although the *x* and *y* crystal dimensions (7 and 4 mm) differed by almost a factor of 2, no significant difference was observed. This behavior is indeed expected because in the first 4 mm of the crystal almost 75% of *z* polarized light has already been absorbed. The use of lower doped (185 and 233 ppm) Cr:KTP confirmed that the absorption of light by Cr^{3+} cations was responsible for the self-diffraction effect. Although the phenomenon of self-diffraction for these doping rates was considerably weaker than for the 677 ppm crystals, the main features described above were also observed.

In order to identify the time scale on which Cr:KTP responds to a laser field at 532 nm, we chopped the laser beam

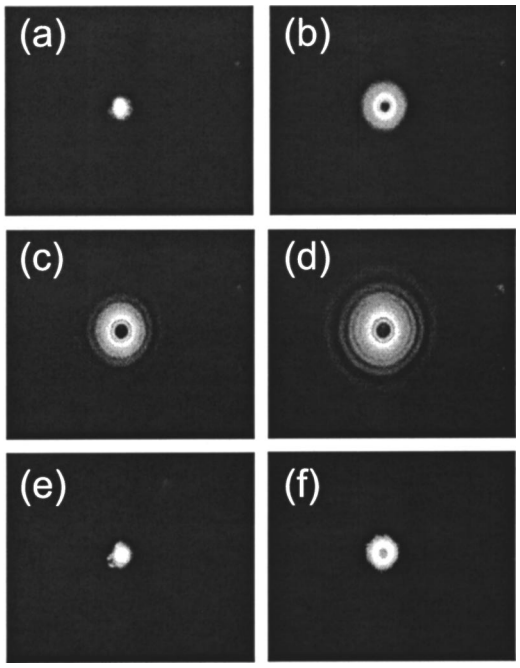

FIG. 3. Diffraction pattern formation in a 677 ppm crystal for a weak laser beam at 633 nm. This probe beam was propagated collinearly with the *z* polarized pump beam along the *y* axis of the crystal. The probe laser was *z* [(a)–(d)] and *x* [(e), (f)] polarized. The pump laser power was [(a), (e)] 200 mW, (b) 750 mW, (c) 1000 mW, (d), (f) 1200 mW.

at different frequencies. The measured outermost ring divergence as a function of this frequency is shown in the inset of Fig. 2 for a *z* polarized laser beam propagating along the *y* axis of a 677 ppm crystal. The incident laser power was 900 mW. An exponential fit to this dependence revealed a response time of about 4 ms. This indicates that the phenomenon of self-diffraction in Cr:KTP is due to a thermo-optical effect.[10]

III. CROSS-PHASE MODULATION

The TEM_{00} output of a HeNe laser at 633 nm with an optical power of 1 mW was used to further investigate the laser-induced refractive index profile in Cr:KTP. The evolution of the diffraction pattern of this probe beam is shown in Figs. 3(a)–3(d) for four different pump powers of 200, 750, 1000, and 1200 mW, respectively. Both beams were *z* polarized and propagated collinearly along the *y* axis of a 677 ppm Cr:KTP sample. Comparing these snapshots with the corresponding self-diffraction patterns from Fig. 1, we see a very pronounced difference. While the pump beam experiences nonlinear interactions with the crystal at extreme light intensities (especially in the self-focus), the probe beam is ''simply'' probing the induced refractive index. Note the dark on-axis spot formation [Figs. 3(b)–3(d)] which implies that the induced refractive index profile appears such that the light rays are repelled from the beam center. In Figs. 3(e) and 3(f) the *x* polarized probe beam diffraction is presented for a collinearly propagating *z* polarized pump with a power of 200 and 1200 mW, respectively. Unlike in Fig. 3(d), the probe beam distortion is much weaker in this case [Fig. 3(f)]. The induced refractive index profile is thus strongly anisotropic, with the highest effect revealed for *z* polarized probe light.

IV. MODELING THE DIFFRACTION PATTERNS

To elucidate the mechanisms underlying the diffraction pattern formation for both the pump and probe beams, a simple theoretical treatment based on a laser heating process and a thermo-optical effect is presented in the following. The equilibrium temperature distribution $\Delta T(\mathbf{r})$ in a medium irradiated with a laser beam with an intensity $I(\mathbf{r})$ is determined by the heat conductance κ and the power density of the heat source $\rho(\mathbf{r})=\alpha I(\mathbf{r})$, where α denotes the fraction of the light intensity which has been absorbed and transferred to thermal excitations. For simplicity, the possible temperature dependence of κ and α is neglected and a linear thermo-optical effect is assumed. Furthermore, since only the relative laser field phase increment affects the beam propagation, the absolute temperature (which is sensitive to the sample shape, heat resistance at edges, etc.) is not considered here. Moreover, for typical conditions in our Cr:KTP experiments, the gradient of $I(\mathbf{r})$ along the laser beam propagation direction is small compared with that along the radial direction *R*. We also assume cylindrical symmetry of the problem (an isotropic heat flow[11] and a transverse laser intensity profile possessing circular symmetry). We note that anisotropy of the diffraction effect arises due to anisotropy in absorption and also in thermo-optical coefficients of the material. Thus, we are left with a one-dimensional steady-state heat flow equation

$$\kappa \frac{1}{R}\frac{\partial}{\partial R}\left[R\frac{\partial \Delta T(R)}{\partial R}\right]=-\alpha I(R), \tag{1}$$

which can easily be integrated for known $I(R)$. After propagating a short distance *d* (thin lens approximation), the variation of the laser phase is given by

$$\Delta\phi(R)=\frac{\omega}{c}n_T\Delta T(R)d, \tag{2}$$

where $n_T=dn/dT$ is the linear thermo-optical coefficient, ω is the light frequency, and *c* is the speed of light. It should be noticed that combining Eqs. (1) and (2) reduces the number of parameters which ''control'' the scaling of $\Delta\phi(R)$ to only one parameter

$$A=\frac{\omega}{c}\frac{P\alpha}{\kappa}n_T d, \tag{3}$$

with *P* denoting the total light power contained in the laser beam. This is because of the fact that in our model *R* is defined in units of W_0. The diffraction pattern (e.g., the number of rings) is solely determined by *A*. However, the outermost ring divergence depends on the ratio λ/W_0, where λ is the wavelength. Now, to calculate the far field diffraction pattern, methods of Fourier optics can be applied.[12] Briefly, the laser beam front acquires a phase shift of $\Delta\phi(R)$ which is determined by numerical evaluation of Eqs. (1) and (2). The Fraunhofer diffraction patterns are then calculated by two-dimensional Fourier transform of this phase shifted laser

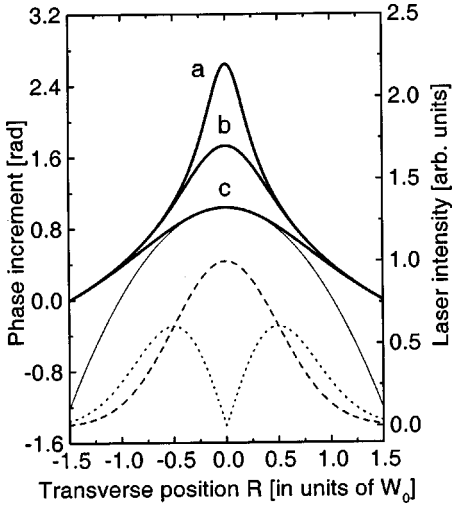

FIG. 4. Calculated laser field phase increments (thick solid lines) for $A/2\pi=1$ and (a) $W_0=0.2$, (b) $W_0=0.5$, and (c) $W_0=1$. Also, the transverse and weighted intensity profiles of the Gaussian pump laser beam are presented for the $1/e^2$ radius $W_0=1$ (dashed and dotted lines, respectively).

field. In the following, the sample is assumed to be located at the laser beam focus where the phase front is plane. Extension to a more general case is straightforward.

The calculated phase increments $\Delta\phi(R)$ in a thin crystal slab irradiated with a Gaussian laser beam

$$I(R)=\frac{2P}{\pi W_0^2}\exp\left(-\frac{2R^2}{W_0^2}\right), \tag{4}$$

where W_0 is the $1/e^2$ beam radius, are presented in Fig. 4 for $A/2\pi=1$ and $W_0=1$, 0.5, and 0.2 (note again that R is measured in W_0), respectively (thick solid lines). Also, the laser beam shape (dashed line) and the ''weighted'' intensity profile[13] (dotted line) are shown for $W_0=1$. We note that in its central part, the temperature profile closely follows a quadratic dependence on R as required for ideal light focusing. This fact is demonstrated in Fig. 4 for $W_0=1$ (thin solid line). However, at $R\simeq W_0/2$, the temperature starts to significantly deviate from this quadratic law. Interestingly, this happens near the maximum of the weighted intensity profile demonstrating that about half of the laser power is used for nonparabolic refractive index modulation. Thus the laser beam phase front becomes essentially nonspherical. It is this last contribution to $\Delta\phi(R)$ which obviously leads to the far field diffraction pattern formation.

In Figs. 5(a) and 5(b) the calculated diffraction patterns are shown for a Gaussian laser beam with $W=W_0$ (self-diffraction) and $A/2\pi=50$ and 100, respectively. However, the intensity distribution in the self-focus does not necessarily need to be Gaussian. In order to demonstrate how the pump beam profile might affect the resulting self-diffraction pattern, Figs. 5(c) and 5(d) show the results for a triangular beam profile with the same choice of $A/2\pi=50$ and 100, respectively.

The Gaussian probe beam diffraction (cross-phase modulation) is shown in Figs. 5(e) and 5(f) for $W=3W_0$, and $A/2\pi=13$ and 50, respectively, for a Gaussian pump beam. In this case the diffraction effect is considerably less

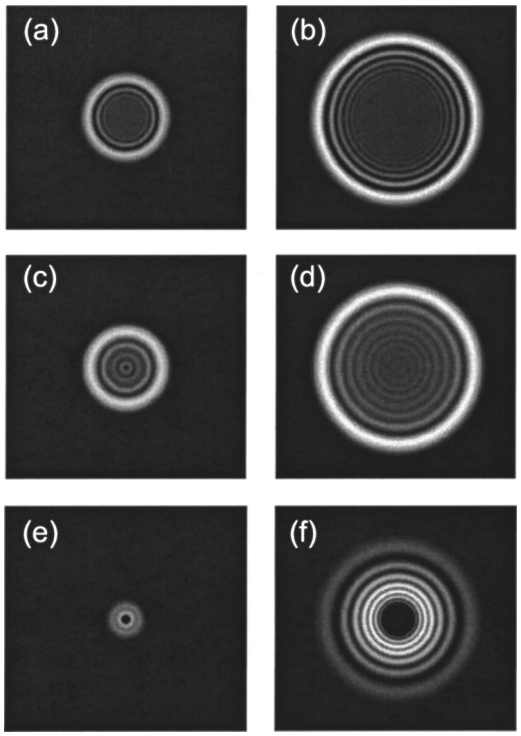

FIG. 5. Calculated far field diffraction patterns. The effect of self-diffraction is demonstrated for $A/2\pi=50$ [(a), (c)] and 100 [(b), (d)] for a Gaussian intensity profile [(a), (b)] and for a triangular beam profile [(c), (d)]. (e) and (f) The diffraction of a Gaussian probe laser beam with $W/W_0=3$ for $A/2\pi=13$ and 50, respectively.

sensitive to the pump beam shape. This fact, as well as the dark on-axis spot formation for the probe beam, is a consequence of the sharp refractive index profile it ''sees'' (see Fig. 4). In contrast, for $W<W_0$, the probe rays would not be repelled from the beam center and a bright central spot would appear. We also note that focusing the same laser power into a smaller spot size results in a much stronger temperature inhomogeneity within the beam (Fig. 4). Therefore, the probe beam diffraction should be more pronounced the smaller the pump diameter. This implies that, although the self-focusing effect arises due to a self-phase modulation in front of the self-focus itself, the largest probe phase modulation, which is essential for efficient diffraction, mostly originates directly from the narrow self-focus region.

V. DISCUSSION

The similarity of the simulated and experimental diffraction patterns indicates that the thin lens approximation is rather satisfactory, at least on a qualitative level. Further improvements of this treatment would result in a more quantitative model which could account for more experimental details and allow for accurate estimation of the third order nonlinear susceptibility of Cr:KTP. First of all, the thick nature of the samples should be considered in order to determine the laser intensity distribution at any longitudinal position. Consequently, the self-diffraction pattern in Cr:KTP could be more accurately reproduced. Also, knowledge of the length and the intensity profile of the self-focus region is essential for making any quantitative conclusions. Neverthe-

less, from the above results we estimate that the largest observed self-induced refractive index change Δn shown in Fig. 1(f) [17 diffraction rings $\Rightarrow A/2\pi = 200$] was approximately $32\lambda/d_f$, where $\lambda = 532$ nm and $d_f \simeq 0.5$ mm are the laser wavelength and the estimated length of the self-focus region, respectively. Thus $\Delta n \simeq 0.04$, corresponding to a maximum temperature change of about 1600 °C ($dn_z/dT = 0.25\times10^{-4}\,\mathrm{K}^{-1}$).[14] More diffraction rings could not be observed because rather violent crystal damage occurred at slightly higher laser powers. We note that the melting point of KTP is 1172 °C. The discrepancy between the estimated temperature change and the melting point is acceptable, bearing in mind the assumptions of our model and its simplicity.

Several authors reported in the past on spatial modulation of a laser beam in KTP.[15–17] In those experiments the buildup of a space-charge field and an electro-optic effect in KTP has been identified as the source of refractive index modulation. This photorefractive effect in KTP has been shown to be extremely anisotropic because of the anisotropy in the ionic conductivities along and perpendicular to the *z* axis of the crystal (10^{-8} and $10^{-12}\,\Omega^{-1}\,\mathrm{cm}^{-1}$, respectively).[15] Moreover, the typical times needed to observe self-induced effects ranged from several minutes[16] to many hours [17] (compare with 4 ms observed in Cr:KTP). In addition, even at laser powers much higher than those applied in our experiments the refractive index has changed considerably less than in Cr:KTP.[17] All these observations lead us to believe that the strong self- and cross-phase modulation effects in Cr:KTP are due to a thermo-optical effect.

VI. CONCLUSIONS

In conclusion, we have shown that incorporation of trivalent cations of Cr into the crystal matrix of KTP induces a high cubic nonlinearity which appears due to a laser heating process and a thermo-optical effect. Extreme light intensities in the self-focus resulted in a pronounced nonparabolic and polarization sensitive refractive index modulation which is at the origin of the diffraction pattern formation. We have also demonstrated that a simple theoretical treatment accounts for the main features observed in the experiments. In addition, the possibility of controlled diffraction of a second laser beam offers exciting opportunities for future applications of Cr:KTP as a material for spatial light modulation.

ACKNOWLEDGMENTS

The authors would like to thank P. Bennema and H. de Haas for their support with crystal growth and J. Hohlfeld, A. J. Quinn, and A. M. Keen for helpful discussions and careful reading of the manuscript. Part of this work was supported by the Stichting voor Fundamenteel Onderzoek der Materie (FOM), which is financially supported by the Nederlandse Organisatie voor Wetenschappelijk Onderzoek (NWO), and by the Stichting Technische Wetenschappen (STW).

[1] J. D. Bierlein and H. Vanherzeele, J. Opt. Soc. Am. B **6**, 622 (1989).
[2] H. Vanherzeele and J. D. Bierlein, Opt. Lett. **17**, 982 (1992).
[3] B. Boulanger, J. P. Fève, G. Marnier, B. Ménaert, X. Cabirol, P. Villeval, and C. Bonnin, J. Opt. Soc. Am. B **11**, 750 (1994).
[4] T. F. McGee, G. M. Blom, and G. Kostecky, J. Cryst. Growth **109**, 361 (1991).
[5] P. A. Morris, A. Ferretti, and J. D. Bierlein, J. Cryst. Growth **109**, 367 (1991).
[6] N.-Y. Chou, E. B. Koker, N. P. Barnes, and G. M. Loiacono, Technical Digest Advanced Solid State Lasers Conference (OSA), MA4-1, 1990.
[7] X. Mu, M. V. Makarov, Y. J. Ding, and J. Wang, 1999 OSA Annual Meeting and Exhibit, TuXX147, 1999.
[8] C. Zaldo, J. Carvajal, R. Solé, F. Diáz, D. Bravo, and A. Kling, J. Appl. Phys. **88**, 3242 (2000).
[9] Y. R. Shen, *The Principles of Nonlinear Optics* (Wiley, New York, 1984), pp. 303–333.
[10] The temperature relaxation time τ can be estimated from the relation $\tau \simeq L^2 c\rho/2\kappa$, where L is the typical length scale in the problem, c is the heat capacity, ρ is the density, and κ is the heat conductivity. Taking $L \simeq 100\ \mu$m (roughly corresponding to our experimental arrangement), and $c = 0.728$ J/gK, $\rho = 3.01$ g/cm^3, and $\kappa_z = 3.3\times10^{-2}$ W/cm K [literature values for undoped KTP (see Ref. 1)], $\tau \simeq 3.3$ ms.
[11] The room temperature thermal conductivity of KTP is anisotropic with the corresponding coefficients along the crystallographic directions $\kappa_x = 2.0\times10^{-2}$, $\kappa_y = 3.0\times10^{-2}$, and $\kappa_z = 3.3\times10^{-2}$ W/cm K (see Ref. 1). This anisotropy would lead to an anisotropic diffraction pattern (astigmatism). Although slight distortion of the patterns is observed in Figs. 1 and 3, they appear considerably more symmetric than expected from the above given thermal conductivities. Actually, at high temperatures required for a thermo-optical diffraction as strong as observed in our experiments, the asymmetry in thermal conductivities can be reduced.
[12] B. A. Saleh and M. C. Teich, *Fundamentals of Photonics* (Wiley, New York, 1991), pp. 109–156.
[13] The quantity $2\pi RI(R)\delta R$ is the laser power contained between R and $R+\delta R$ and is referred to as the weighted intensity profile.
[14] W. Wiechmann, S. Kubota, T. Fukui, and H. Masuda, Opt. Lett. **18**, 1208 (1993).
[15] H. Yang, S. Gu, Z. Xu, Y. Zhu, and Y. Li, Phys. Rev. B **37**, 1161 (1988).
[16] L. P. Shi, W. Karthe, and A. Rasch, Appl. Phys. Lett. **65**, 2539 (1994).
[17] J. K. Tyminski, J. Appl. Phys. **70**, 5570 (1991).